Sustained CGRP1 receptor stimulation modulates development of EC coupling by cAMP/PKA signalling pathway in mouse skeletal myotubes

Guillermo Avila, Citlalli I. Aguilar and Roberto Ramos-Mondragón

Departamento de Bioquímica, Cinvestav-IPN, AP 14-740, México, DF 07000, México

We investigated modulation of excitation–contraction (EC) coupling by calcitonin gene-related peptide (CGRP), which is released by motorneurons during neuromuscular transmission. Mouse skeletal myotubes were cultured either under control conditions or in the presence of 100 nM CGRP (∼4–72 h). T- and L-type Ca^{2+} currents, immobilization resistant charge movement, and intracellular Ca^{2+} transients were characterized in whole-cell patch-clamp experiments. CGRP treatment increased the amplitude of voltage-gated Ca^{2+} release ($(\Delta F/F)_{max}$) ∼75–350% and moderately increased both maximal L-current conductance (G_{max}) and charge movement (Q_{max}). In contrast, CGRP treatment did not affect their corresponding voltage dependence of activation ($V_{1/2}$ and k) or T-current density. CGRP treatment enhanced voltage-gated Ca^{2+} release in ∼4 h, whereas the effect on L-channel magnitude took longer to develop (∼24 h), suggesting that short-term potentiation of EC coupling may lead to subsequent long-term up-regulation of DHPR expression. CGRP treatment also drastically increased caffeine-induced Ca^{2+} release in ∼4 h (∼400%). Thus, short-term potentiation of EC coupling is due to an increase in sarcoplasmic reticulum Ca^{2+} content. Both application of a phosphodiesterase inhibitor (papaverine) and a membrane-permeant cAMP analogue (Db-cAMP) produced a similar potentiation of EC coupling. Conversely, this potentiation was prevented by pretreatment with either CGRP1 receptor antagonist ($CGRP_{8-37}$) or a PKA inhibitor (H-89). Thus, CGRP acts through CGRP1 receptors and the cAMP/PKA signalling pathway to enhance voltage-gated Ca^{2+} release. Effects of CGRP on both EC coupling and L-channels were attenuated at later times during myotube differentiation. Therefore, we conclude that CGRP accelerates maturation of EC coupling.

(Received 30 May 2007; accepted after revision 25 July 2007; first published online 26 July 2007)
Corresponding author G. Avila: Departamento de Bioquímica, Cinvestav-IPN, AP 14–740, México, DF 07000, México. Email: gavila@cinvestav.mx

In skeletal muscle, excitation–contraction (EC) coupling is under the control of voltage sensors of the transverse tubules (Schneider & Chandler, 1973). The molecular identity of the voltage sensor is the α_1-subunit of the voltage-dependent L-type Ca^{2+} channels (L-channels), also known as the dihydropyridine receptor or DHPR (Rios & Brum, 1987; Tanabe *et al.* 1988). The DHPRs are believed to be physically bound to ryanodine receptors or RyR1s (Marty *et al.* 1994), which are intracellular Ca^{2+} release channels located at the sarcoplasmic reticulum (SR). In response to sarcolemmal depolarization, DHPRs activate nearby RyR1s, producing a massive release of Ca^{2+} from the SR and a brief increase in intracellular Ca^{2+} concentration (termed a Ca^{2+} transient). This increase in intracellular Ca^{2+} subsequently activates proteins of the contractile machinery, ultimately resulting in muscle contraction (for reviews see Melzer *et al.* 1995; Dirksen, 2002).

Calcitonin gene-related peptide (CGRP) is a 37-amino-acid neuropeptide that is synthesized and released by motor neurons at the neuromuscular junction during skeletal muscle development (Matteoli *et al.* 1990). CGRP binds to at least two classes of membrane receptors (CGRP1 and CGRP2), which are positively coupled to G_s proteins and activation of adenylate cyclase (Juaneda *et al.* 2000; Hay *et al.* 2003). The 30 amino acid variant of CGRP, $CGRP_{8-37}$, is commonly used as a selective antagonist of the CGRP1 receptor (Chiba *et al.* 1989). CGRP released from motor neuron terminals following electrical stimulation (Uchida *et al.* 1990; Sakaguchi *et al.* 1991; Sala *et al.* 1995) binds to membrane receptors of skeletal muscle (Fernandez *et al.* 2003; Rossi *et al.*

 DOI: 10.1113/jphysiol.2007.137687

2003). Activation of muscle CGRP receptors increases contraction force and the activity of the Na^+/K^+ pump via increasing levels of cyclic-adenosine monophosphate (cAMP) generation and subsequent protein kinase A (PKA) activation (Takami *et al.* 1985; Takami *et al.* 1986; Uchida *et al.* 1990; Andersen & Clausen, 1993).

In developing skeletal muscle (i.e. myotubes and/or cultured embryonic/neonate muscle fibres), CGRP increases the rate of acetylcholine receptor (AchR) desensitization (Mulle *et al.* 1988), potentiates AChR channel activity (Lu *et al.* 1993), increases the number of AChRs (Fontaine *et al.* 1986; New & Mudge, 1986), and decreases acetylcholinesterase expression (Boudreau-Lariviere & Jasmin, 1999; Rossi *et al.* 2003). Nevertheless, the role of CGRP in modulating skeletal muscle EC coupling remains unexplored, even though this process is critical in determining force generation.

Skeletal myotubes represent a widely used experimental model to investigate the molecular and cellular mechanisms of EC coupling. Myotubes are small and electrically compact, which is required to ensure adequate voltage clamp in whole-cell patch-clamp experiments (Beam & Franzini-Armstrong, 1997).

In the present study, we demonstrate that CGRP modulates development of EC coupling in skeletal myotubes. We determined the involvement of the following downstream molecules in the CGRP response: CGRP1 receptors, cAMP and PKA. Our results indicate that CGRP exposure activates a CGRP receptor–cAMP–PKA pathway that accelerates maturation of the EC coupling 'machinery' by enhancing SR Ca^{2+} content, voltage-gated SR Ca^{2+} release, and the density of sarcolemmal DHPRs.

Methods

Primary cultures of myotubes

Primary cultured myotubes were obtained as described in Mejia-Luna & Avila (2004). Animal manipulations were performed according to the Mexican Official Norm NOM-062-ZOO-199 and the *Guide for the Care and Use of Laboratory Animals* as adopted of the National Institutes of Health (USA). Briefly, newborn mice were decapitated and skeletal muscle myoblasts were isolated from forelimb and hindlimb muscles. Muscle was removed, digested with trypsin (at 37°C, 45 min) and then mechanically dispersed. The resulting preparation was filtered and preplated to decrease fibroblast content. Semipurified myoblasts were then plated on sterile glass coverslides (8000 cells cm^{-2}) placed in 35 mm Petri dishes. Myoblasts were allowed to proliferate for 24 h in plating medium, which consisted of Dulbecco's modified Eagle's medium (DMEM) supplemented with 10% horse serum (HS), 100 U ml^{-1} penicillin, 100 μg ml^{-1} streptomycin and 4 mM L-glutamine. Experiments were performed in cultures 3–6 days after exchanging plating medium with fusion medium, which was similar to the plating medium but only contained 2% HS (as opposed to 10%).

Exposure of myotubes to CGRP, caffeine and other compounds

Myotubes were initially grown for 3 days in fusion medium. Afterwards cells either remained in the standard fusion medium (control myotubes) or were cultured in fusion medium supplemented with either 100 nM CGRP (α-CGRP; rat, synthetic) or other compounds (Db-cAMP, H-89, $CGRP_{8-37}$) as indicated. Fusion medium in all experiments was subsequently replenished every 24 h. Control traces in all figures represent myotubes cultured in standard fusion medium for the same additional period of time as that used for treated myotubes (i.e. time-matched controls). Except for caffeine, myotubes were not exposed to CGRP or other compounds during patch-clamp experiments, which were performed ~15–90 min following removal of medium.

Caffeine (30 mM) was locally applied under whole-cell patch-clamp conditions by gravity using a custom-made fast perfusion system. Applications were performed ~20 s after brief depolarizing steps delivered from a holding potential of −80 mV (30 ms to +70 mV). Caffeine was dissolved in a rodent Ringer solution consisting of (mM): 145 NaCl, 5 KCl, 2 $CaCl_2$, 1 $MgCl_2$, and 10 4-(2-hydroxyethyl)-1-piperazineethanesulphonic acid (Hepes); pH 7.4 with NaOH.

Measurements of ionic and gating currents

Ionic and gating currents were measured using the whole-cell mode of the patch-clamp technique, as previously described (Mejia-Luna & Avila, 2004). Briefly, a coverslide of myotubes was withdrawn from a Petri dish containing fusion medium and transferred to a recording chamber filled with extracellular recording solution (see Recording solutions). Myotubes were observed through an IX71 inverted microscope (Olympus America Inc., Melville, NY, USA) and patch-clamp experiments were conducted within the next ~15–90 min using an Axopatch 200B amplifier, a Digidata 1322A digitizer (Axon Instruments Inc., Union City, CA, USA), and pCLAMP 9.2 software (Axon Instruments) installed on a personal computer (1.6 GHz CPU, Compaq/Hewlett-Packard). Sampling frequencies were 5 kHz and 50 kHz, for ionic and gating currents, respectively. Whole-cell patch clamp electrodes exhibited electrical resistances of ~2.0 MΩ when filled with the internal solution (see Recording solutions). The patch electrodes were fabricated from borosilicate glass capillaries using a two-stage vertical puller (L/M-3P-A, List-Electronik, Darmstadt/Elberstadt,

Germany) and a MF-830 microforge (Narishige International USA, Inc., Long-Island, NY, USA). Total cell membrane capacitance (C_m) and series resistance (R_s) were estimated, analogically cancelled, and the remaining linear components digitally removed using a p/N ($n = -3$) online subtraction protocol. If necessary, R_s was compensated (~40–85%) to ensure a time constant for charging the membrane capacitance (τ) of 100–300 μs. Investigated myotubes typically exhibited C_m values of ~70–300 pF. Ca^{2+} currents were elicited by 200 ms pulses of variable amplitude, in the absence (T- and L-type Ca^{2+} currents) or the presence (L-type Ca^{2+} current) of a 1 s prepulse to −30 mV (followed by 50 ms at −50 mV). The holding potential (HP) was −80 mV. All current signals were normalized by C_m. In some cases outward gating currents and inward tail currents are truncated for clarity. Peak L-type Ca^{2+} current density at the end of each 200 ms pulse was plotted as a function of membrane potential and fitted according to:

$$I = G_{max}(V_m - V_{rev})/(1 + \exp\{[V_{1/2,G} - V_m]/k_G\}) \quad (1)$$

Where G_{max} is the maximal L-channels conductance, V_m is the test potential, V_{rev} is the extrapolated reversal potential, $V_{1/2,G}$ represents the voltage for half-maximal conductance activation, and k_G is a slope factor.

Immobilization-resistant intramembrane charge movement was measured as described by Avila *et al.* (2001). Test pulses were applied following the prepulse protocol described above in the presence of extracellular Cd^{2+} (0.5 mM) and La^{3+} (0.2 mM). The amount of charge movement was estimated by integrating outward nonlinear capacitive currents after onset of the test pulse (Q_{ON}). Immobilization-resistant charge movement (Q_{ON}) was plotted as a function of membrane potential and fitted according to the following equation:

$$Q_{ON} = Q_{max}/(1 + \exp[(V_{1/2,Q} - V_m)/k_Q]) \quad (2)$$

where Q_{max}, V_m, $V_{1/2,Q}$ and k_Q have their usual meanings with regard to charge movement.

Measurements of Ca^{2+} transients

Intracellular Ca^{2+} transients were measured as previously described (Avila *et al.* 2001). Briefly, myotubes were transferred from the incubator to an extracellular recording solution (see Recording solutions) and subjected to whole-cell voltage-clamp experiments, as described above. In this case, the internal recording solution was supplemented with 0.2 mM of the Ca^{2+} sensitive (free-acid) dye fluo-4 (K_5fluo-4; see Recording solutions). Emitted fluo-4 fluorescence was acquired from a small rectangular area of the investigated myotube, which did not include the patch pipette. Extracellular fluorescence (due to dye leak from the pipette prior to seal formation) was eliminated by perfusing excess of external solution. Fluo-4 was excited using a 100 W mercury arc lamp. The excitation cube (U-MNIBA, Olympus America Inc.) consisted of the following elements: dichroic mirror (505 nm), excitation filter (470–490 nm bandwidth), and emission filter (515–550 nm bandwidth). Except for experiments where myotubes were exposed to caffeine, depolarizing pulses (of 30 ms) were applied following the prepulse protocol used to inactivate T-type Ca^{2+} channels (see previous section). A computer-controlled shutter (Vincent Associates, Rochester, NY, USA) was used to block illumination during interpulse intervals. The fluorescence signal was acquired using a photomultiplier detection system (Photon Technology International, Inc.; Birmingham, NJ, USA) working in the analog mode, digitized, and stored for subsequent offline analysis. Sampling frequencies were 2 kHz and 10 kHz, for caffeine- and voltage-gated Ca^{2+} transients, respectively. Relative changes in intracellular Ca^{2+} are expressed as fluorescence change (ΔF) divided by basal fluorescence (F) observed just before stimulation ($\Delta F/F$). The amplitude of voltage-gated Ca^{2+} transients measured at the end of test pulses was plotted as a function of membrane potential and fitted according to:

$$\Delta F/F = (\Delta F/F)_{max}/1 + \exp[(V_{1/2,F} - V_m)/k_F]) \quad (3)$$

where $(\Delta F/F)_{max}$, $V_{1/2,F}$, V_m, and k_F have their usual meanings with regard to Ca^{2+} transients. The peak of the first derivative of $\Delta F/F$ was used as an indirect measure of the maximal rate of SR Ca^{2+} release (as described in Avila & Dirksen, 2005).

Recording solutions

All ionic and gating current measurements were performed in the presence of the following external recording solution (mM): 145 tetraethylamonium-Cl (TEA-Cl), 10 $CaCl_2$, 0.003 tetrodotoxin (TTX) and 10 Hepes. Immobilization-resistant intramembrane charge movement was measured following block of Ca^{2+} currents by supplementing the external solution with 0.5 mM $CdCl_2$ and 0.2 mM $LaCl_2$. Ionic and gating current measurements were recorded using the following internal solution (mM): 135 caesium aspartate, 10 caesium ethylene glycol tetraacetic acid (Cs_2EGTA), 5 $MgCl_2$ and 10 Hepes. Intracellular Ca^{2+} transients were measured using an internal solution that consisted of (mM): 145 caesium aspartate, 10 CsCl, 0.1 Cs_2EGTA, 1.2 $MgCl_2$, 5 MgATP, 0.2 fluo-4 pentapotassium (K_5Fluo-4), and 10 Hepes. The pH of all solutions was adjusted to 7.4. All measurements were carried out at room temperature (22–24°C).

Statistical analysis

All results are expressed as means ± S.E.M. and were analysed using Microsoft Excel, pCLAMP 9.2 (Axon Instruments), and SigmaStat 3.5 (Systat Software Inc., San Jose, CA, USA) software. Significant differences were determined at the $P < 0.05$ level unless otherwise specified. One-way analysis of variance (ANOVA) was used when comparisons involved more than two experimental conditions (Fig. 7). Two-way ANOVA was used to examine the effects of CGRP as a function of time in culture (Figs 2 and 4). Pairs of means were compared *post hoc*, using the Holm–Sidak method. Other statistical comparisons were performed using Student's *t* test for unpaired data.

Results

CGRP enhances voltage-gated SR Ca^{2+} release

We first aimed to investigate whether voltage-gated Ca^{2+} release in myotubes is regulated by chronic treatment with CGRP. To this end, myotubes were exposed to 100 nM CGRP for 1–3 days, and then Ca^{2+} transients were elicited in response to short (30 ms) membrane depolarizations. Figure 1*A* shows representative Ca^{2+} transient traces elicited at various membrane potentials (from −10 mV to +70 mV). Clearly, Ca^{2+} transient amplitude is drastically enhanced following 1–3 day exposure to CGRP. On average, CGRP increased the Ca^{2+} transient amplitude ($(\Delta F/F)_{max}$) 120% (Fig. 1*B*, and Table 1). However, the other parameters of the voltage dependence of Ca^{2+} release (k_F and $V_{1/2,F}$) were not significantly altered (Fig. 1*C* and Table 1).

Table 1. Parameters of fitted Δ*F*/*F*–*V*, *G*–*V*, and *Q*–*V* curves

	Control	CGRP
Δ*F*/*F*–*V*		
$(\Delta F/F)_{max}$	1.0 ± 0.2	2.2 ± 0.2*
k_F (mV)	7.4 ± 0.7	7.8 ± 0.5
$V_{1/2,F}$ (mV)	8.6 ± 1.9	9.4 ± 1.3
n	20	21
G–*V*		
G_{max} (nS nF^{-1})	288 ± 11	344 ± 11*
k_G (mV)	5.9 ± 0.1	5.9 ± 0.1
$V_{1/2,G}$ (mV)	18.2 ± 0.4	17.9 ± 0.5
V_{rev} (mV)	79.2 ± 0.7	80.9 ± 0.6
n	54	40
Q–*V*		
Q_{max} (nC μF^{-1})	8.8 ± 0.5	11.0 ± 0.8*
k_Q (mV)	9.9 ± 0.4	9.5 ± 0.3
$V_{1/2,Q}$ (mV)	12.9 ± 1.2	11.2 ± 1.3
n	15	15

Average values (mean ± S.E.M.) of voltage dependent parameters obtained by fitting results from each particular myotube according to the Boltzmann equations described in Methods (eqns (1)–(3)). *$P < 0.05$, compared to control.

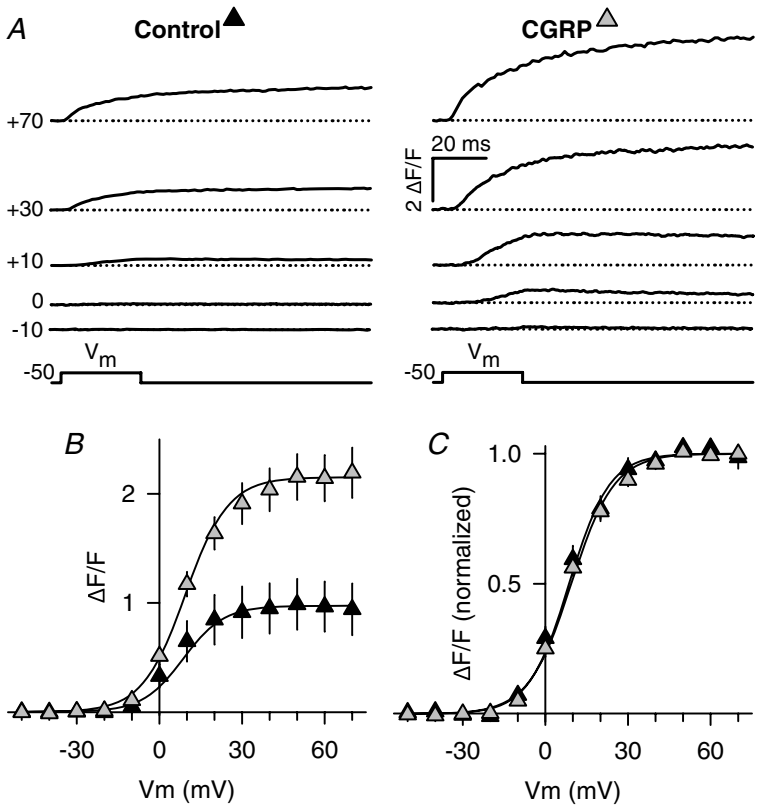

Figure 1. Effects of CGRP on voltage-gated Ca^{2+} transients
A, representative voltage-gated Ca^{2+} transients obtained from control (left) and CGRP-treated (right) myotubes. Test pulses (V_m) to the indicated voltages (shown in left margin) were elicited following 1 s prepulses used to inactivate T-type Ca^{2+} currents (see Methods). *B*, average voltage dependence of Ca^{2+} transients elicited as in *A*. Ca^{2+} transient amplitude measured at the end of each test pulse is plotted as a function of V_m. Continuous lines represent fitted Δ*F*/*F*-values obtained using eqn (3) and the resulting average Boltzmann parameters reported in Table 1. *C*, normalized voltage dependence of Ca^{2+} transients. Absolute Δ*F*/*F* values from each myotube were normalized by their corresponding maximal value and plotted as a function of V_m. Results were obtained from 20 control (black triangles) and 21 CGRP-treated (grey triangles) myotubes. CGRP treatment was 100 nM for 1–3 days.

The increase in the amplitude of the Ca^{2+} transient could result from an increase in the rate of voltage-gated SR Ca^{2+} release. Thus, we calculated the peak of the first derivative of $\Delta F/F$ (i.e. dF/dt), which represents a reasonable approximation of the maximum rate of SR Ca^{2+} release (Avila & Dirksen, 2005). CGRP was found to significantly increase the maximum dF/dt by ∼90%, from 97 ± 17 to 184 ± 25 $\Delta F/F\ s^{-1}$ ($P < 0.01$, same cells as in Fig. 1).

To investigate the onset of Ca^{2+} transient potentiation by CGRP, we determined $(\Delta F/F)_{max}$ in myotubes treated from ∼1 h to up to ∼79 h compared to that of time-matched controls. The experimental results were subsequently pooled as follows: ∼1–7 h (4 h), ∼24–31 h (1 day), ∼48–55 h (2 days), and ∼72–79 h (3 days). Figure 2*A* shows representative Ca^{2+} transients recorded from each time point (time in days is indicated in italic numbers). The corresponding average values of $(\Delta F/F)_{max}$ are shown in Fig. 2*B*. Under control conditions, these values grow steadily between 0 and 3 days (from ∼0.7 $\Delta F/F$, to up to ∼1.7 $\Delta F/F$). In contrast, CGRP-treated myotubes exhibit a marked increase in voltage-gated Ca^{2+} release even as early as 4 h post-exposure, a similar magnitude as that observed for control myotubes after 3 days in control medium. However, voltage-gated Ca^{2+} release does not significantly increase further even following 3 days of CGRP exposure. These data suggest that CGRP accelerates the development of voltage-gated SR Ca^{2+} release in culture.

CGRP selectively increases L-channel expression

The results shown in Figs 1 and 2 prompted us to investigate whether CGRP enhancement of voltage-gated SR Ca^{2+} release might involve a possible effect on voltage-gated Ca^{2+} channels. Figure 3 shows L-type (Fig. 3*B* and *D*) and total Ca^{2+} currents (i.e. T-type plus L-type, Fig. 3*A* and *C*) in control and CGRP-treated myotubes (1–3 days). As can be seen from both the representative currents (Fig. 3*A* and *B*) and average *I–V* curves (Fig. 3*C* and *D*), CGRP significantly increased the L-type Ca^{2+} current density by ∼25% ($P < 0.0005$ at +30 mV), while not significantly affecting T-type Ca^{2+} current density ($P = 0.2$ at −30 mV). The increase in L-type Ca^{2+} current density was entirely explained by a selective effect on the maximal L-channels conductance (G_{max}), the only parameter of the Boltzmann fit (eqn (1)) that was significantly altered (see Table 1).

We next set out to investigate the time course for the observed effect on G_{max} in a similar way as shown for Ca^{2+} transients in Fig. 2. An important difference, however, was that the shortest treatment we investigated for the L-type Ca^{2+} current was 0.5 days (∼8–15 h treatments), as opposed to 0.15 days for Ca^{2+} release (Fig. 2). Thus, we compared L-type Ca^{2+} current density in time-matched control and CGRP-treated myotubes (Fig. 4). The results indicate that L-current density was significantly increased 1–2 days following CGRP treatment, but not following 0.5 or 3 days. Thus, similar to that observed for voltage-gated Ca^{2+} release, the CGRP-induced increase in L-current density is also diminished after several days in culture. However, more importantly, the increase of L-type Ca^{2+} current density occurred only after a significant delay (∼1 day) compared to that observed for potentiation of voltage-gated Ca^{2+} release (∼4 h).

We next investigated whether the CGRP-induced enhancement in L-current density results from an increase in the number of voltage sensors in the

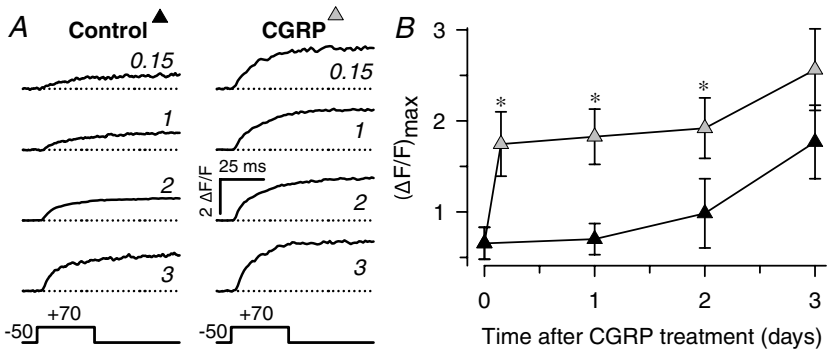

Figure 2. Time course of CGRP effect on voltage-gated Ca^{2+} transients
A, representative voltage-gated Ca^{2+} transients obtained from myotubes cultured for 0–3 days either under control conditions (left) or in the presence of 100 nM CGRP (right). Ca^{2+} transient amplitude was estimated as described in Fig. 1. The approximated time (in days) following initiation of treatment is indicated with italicized numbers. *B*, average amplitude of voltage-gated Ca^{2+} transients ($(\Delta F/F)_{max}$) obtained at different times after CGRP treatment (100 nM). Results were obtained from 6 to 12 myotubes for each condition. $(\Delta F/F)_{max}$ was estimated by either fitting experimental data to eqn (3) or averaging peak $\Delta F/F$ values obtained at saturating voltages (+30 mV to +70 mV). Results from two-way ANOVA and *post hoc* Holms–Sidak test indicated significant differences between control and CGRP-treated groups (*$P \leq 0.05$). Specifically, the *P* values between CGRP-treated and time-matched controls obtained for 0.15, 1, 2, and 3 day treatments were 0.021, 0.008, 0.050, and 0.086, respectively.

sarcolemma. Specifically, we compared the amount of immobilization-resistant intramembrane charge movement between control and CGRP-treated (1–3 days) myotubes. Charge movement magnitude was estimated by integrating the nonlinear capacitive (gating) currents elicited at the onset of membrane depolarization (Q_{ON}). Figure 5*A* shows representative gating currents obtained from control (left) and CGRP-treated (right) myotubes. Gating currents were significantly larger in CGRP-treated myotubes. In fact, CGRP increased the maximal magnitude of Q_{ON} (Q_{max}; Fig. 5*B*) without significantly altering the steepness (k_Q) or voltage distribution ($V_{1/2,Q}$) of the charge movement–voltage relationship (Fig. 5*C*). Thus, the observed increase in Q_{ON} (∼25%) is sufficient to account for a similar 25% increase in G_{max} observed in Figs 3 and 4.

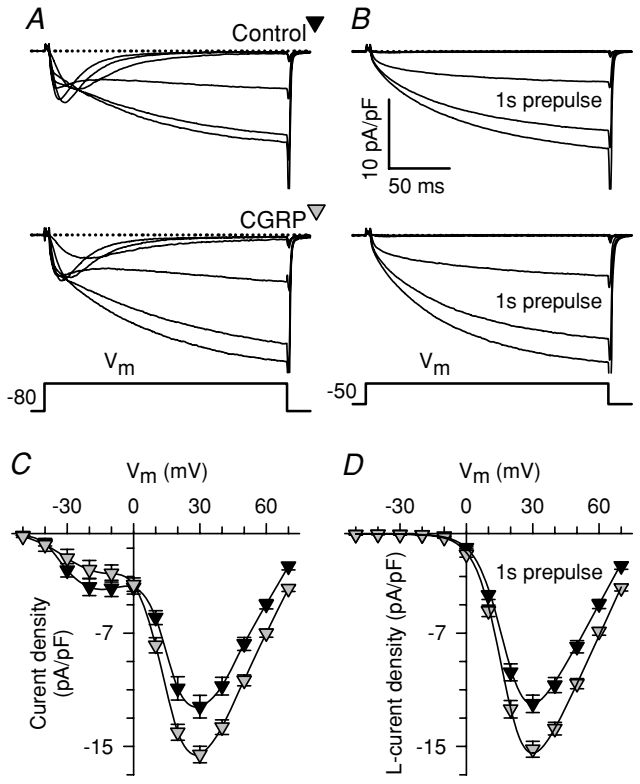

Figure 3. CGRP selectively increases L-type Ca^{2+} current density
A and *B*, representative traces of total (*A*) and L-type (*B*) Ca^{2+} currents obtained from control (top) and CGRP-treated (bottom) myotubes. Total (T-type and L-type) Ca^{2+} currents were first elicited from the holding potential (−80 mV). Subsequently, a family of L-type Ca^{2+} currents were elicited following a 1 s prepulse to −30 mV to inactivate T-type Ca^{2+} channels. Ca^{2+} current traces are shown for the following membrane potentials (mV): −20, −10, 0, +10, +20 and +30. *C* and *D*, average current–voltage relationships (*I–V* curves) obtained for total (*C*) and L-type (*D*) Ca^{2+} currents. Results were obtained from 31 (*C*) and 54 (*D*) control myotubes (black triangles), and 29 (*C*) and 40 (*D*) CGRP-treated myotubes (1–3 days, 100 nM; grey triangles). The continuous lines in *D* represent fits to the data using eqn (1) and average values of the parameters of these fits are shown in Table 1 (*G–V* data). A spline curve was used to generate the smooth lines through the data in *C*.

CGRP increases SR Ca^{2+} content

While an increase in charge movement is sufficient to explain a parallel increase in L-type Ca^{2+} current density (∼1.25-fold increase in both measurements), the slower time course of this effect makes it unlikely to account for an even larger effect on voltage-gated Ca^{2+} release (∼2.2-fold increase in only 4 h). Thus, we speculated that potentiation of Ca^{2+} release may involve an increase in luminal SR Ca^{2+} content. To test this possibility, we compared the caffeine-releasable Ca^{2+}-releasable pool in control and 4 h CGRP-treated myotubes (i.e. prior to a change in L-type Ca^{2+} current). Specifically, we measured the amplitude of Ca^{2+} transients induced by caffeine (30 mM), a widely used ryanodine receptor agonist, under identical conditions as those used to assess voltage-gated Ca^{2+} release (i.e. measurements of both voltage- and caffeine-induced Ca^{2+} transients on the same myotube, Fig. 6). In both, control and CGRP-treated myotubes, caffeine application produced a relatively fast increase in intracellular Ca^{2+} concentration whose maximal amplitude was higher than the peak Ca^{2+} transient elicited by voltage (Fig. 6).

In this set of experiments we used higher concentrations of CGRP (100–300 nM, as opposed to 100 nM), and voltage-gated Ca^{2+} release was stimulated to an even larger degree (3.5-fold; Fig. 6, Voltage). The larger effect on voltage-gated Ca^{2+} release in these experiments could be explained by the use of a higher CGRP concentration. However, a somewhat smaller effect on voltage-induced release (∼2.3-fold) was observed using 100–300 nM CGRP in a separate set of experiments (Fig. 7, culture 3). This apparent contradiction may deserve further investigation. In any event, 100–300 nM CGRP-treated myotubes exhibited a remarkable increase (4.0-fold) in the peak amplitude of caffeine-induced Ca^{2+} release (Fig. 6*B*, Caffeine). Moreover, the ratios of Ca^{2+} release induced by caffeine and voltage (i.e. caffeine-to-voltage ratio) were not statistically different for control (1.1 ± 0.2) and CGRP-treated (1.3 ± 0.2) myotubes. These results indicate that CGRP drastically enhances the magnitude of the caffeine-releasable Ca^{2+}-releasable pool, an effect that is sufficient to explain the corresponding potentiation of voltage-gated SR Ca^{2+} release.

Potentiation of Ca^{2+} release by CGRP is mediated by CGRP1 receptor signalling through cAMP/PKA

CGRP binds to at least two different membrane receptors, CGRP1 and CGRP2, and blockade of CGRP effects by $CGRP_{8-37}$ defines a CGRP1 receptor mediated response (Chiba *et al.* 1989; reviewed by Juaneda *et al.* 2000). Thus,

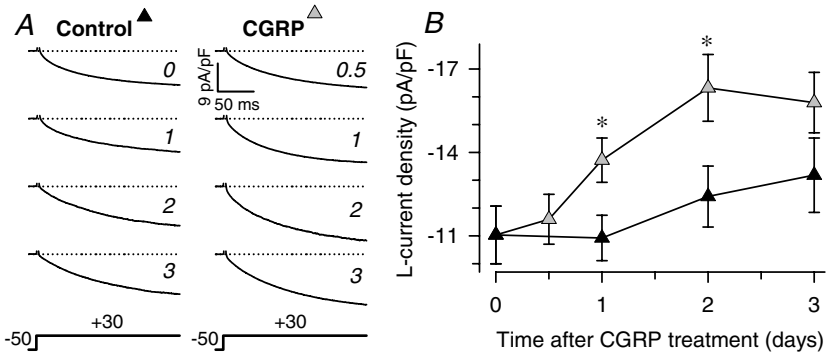

Figure 4. Time course of CGRP-mediated increase in L-type Ca^{2+} current density
A, representative L-type Ca^{2+} currents from myotubes cultured for 0–3 days in either the absence (left) or the presence of 100 nM CGRP (right). The time after initiation of CGRP treatment (in days) is shown in italicized numbers. Current traces were elicited using 200 ms depolarizing pulses to +30 mV that were preceded by a 1 s prepulse to inactivate T-type Ca^{2+} channels. *B*, time course of average peak L-type Ca^{2+} current density obtained from control (black triangles) and CGRP-treated (grey triangles) myotubes. Data represent means ± S.E.M. from 12–19 myotubes for each condition. Two-way ANOVA indicates significant differences between control and CGRP-treated (100 nM) groups ($P < 0.002$). The *P*-values obtained from *post hoc* Holms–Sidak tests between time-matched control and CGRP-treated for 0.5, 1, 2 and 3 days of treatment were 0.700, 0.049, 0.036 and 0.069, respectively. $^*P < 0.05$.

we investigated the possibility that CGRP potentiation of voltage-gated SR Ca^{2+} release might be mediated by signalling through a CGRP1 receptor. We found that $CGRP_{8-37}$ blocks CGRP stimulation of voltage-gated SR Ca^{2+} release (Fig. 7, Culture 1). These results indicate that CGRP augments voltage-gated Ca^{2+} release by acting through CGRP1 receptors.

CGRP1 receptors couple via G_s proteins to stimulate adenylate cyclase leading to the generation of cAMP and activation of PKA (Juaneda *et al.* 2000; Hay *et al.* 2003). Thus we next investigated the role of the cAMP/PKA signalling pathway in the CGRP enhancement of voltage-gated SR Ca^{2+} release. To this end, we preincubated myotubes with 10 μM H-89, a specific inhibitor of PKA, for ∼60 min prior to CGRP exposure. Interestingly, the stimulatory effect of CGRP was completely inhibited by H-89 pretreatment (Fig. 7, Culture 2), similarly to that observed for $CGRP_{8-37}$. Thus, CGRP requires PKA to potentiate voltage-gated SR Ca^{2+} release.

The next step was to investigate a possible contribution of cAMP. To achieve this goal, we used two different pharmacological approaches. We first investigated whether the effect of CGRP could be mimicked by Db-cAMP, a membrane-permeant cAMP analogue. As can be observed in Fig. 7 (Culture 3), Db-cAMP exposure also increased the amplitude of voltage-gated Ca^{2+} release, albeit to a somewhat lesser degree than CGRP. We also preincubated myotubes with papaverine, a nonselective inhibitor of phosphodiesterases, which promotes cAMP accumulation by inhibiting its degradation. Papaverine treatment produced a 2.6-fold increase in the amplitude of voltage-gated Ca^{2+} release (Fig. 7, PAP), similar to the effect seen with CGRP. Representative voltage-gated Ca^{2+} transients elicited at +70 mV are shown in Fig. 7*B*. Other myotubes were treated with papaverine plus Db-cAMP

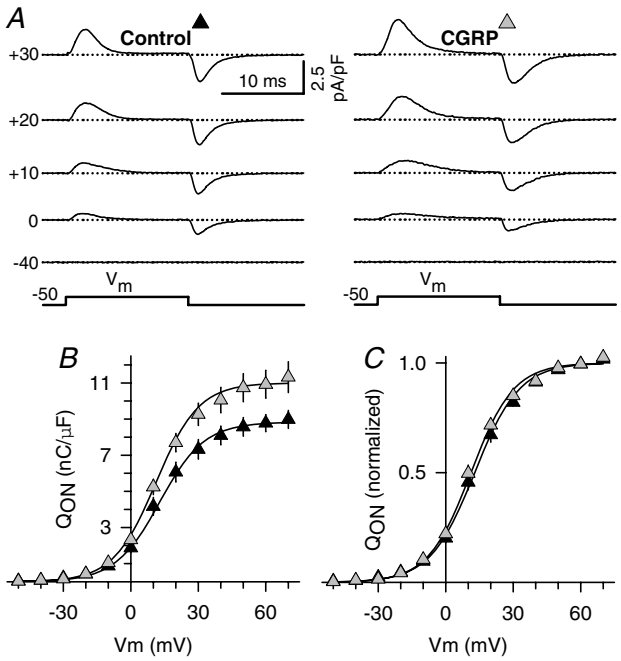

Figure 5. CGRP increases immobilization-resistant charge movement
A, representative non-capacitative gating currents (asymmetric charge movements) obtained from control (left) and CGRP-treated (right) myotubes elicited at different membrane potentials (left margin). *B*, average voltage dependence of asymmetric charge movement estimated from integrating the non-capacitative current during the onset of each test depolarization (Q_{ON}) plotted as a function of V_m. The continuous lines through the data were generated by fitting each data set with eqn (2). Average values of the fitted parameters are shown in Table 1 (*Q–V* data). *C*, normalized voltage dependence of charge movement. Absolute values of Q_{ON} obtained from each myotube were normalized by their corresponding maximum values (Q_{max}), averaged, and plotted as a function of V_m. Experimental results were obtained from 15 control (black triangles) and 15 CGRP-treated (1–3 days, 100 nM; grey triangles) myotubes.

(Fig. 7, Culture 4), in order to determine whether these two agents exert an additive effect on release. However, combined treatment with papaverine and Db-cAMP failed to further increase voltage-gated Ca^{2+} release. These results indicate that cAMP stimulates voltage-gated SR Ca^{2+} release. Taken together, results presented in Fig. 7 indicate that potentiation of SR Ca^{2+} release by CGRP is mediated by activation of the CGRP1 receptor, production cAMP, and subsequent stimulation of PKA.

Discussion

This study represents to our knowledge the first demonstration that CGRP regulates the development of the EC coupling machinery in skeletal muscle. We discovered that CGRP markedly stimulates voltage-gated SR Ca^{2+} release. The intensity of this effect varies between 1.7- and 3.5-fold, across different experimental series. We also found that stimulation of voltage-gated SR Ca^{2+} release results primarily from a significant increase in the SR Ca^{2+} content, and does not involve alterations in the voltage dependence of the release process. Additionally, this work points to a critical role for the activation of

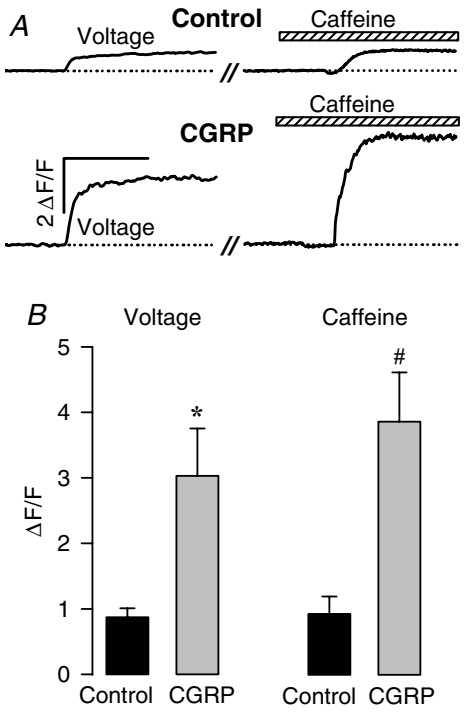

Figure 6. CGRP similarly potentiates voltage- and caffeine-induced SR Ca^{2+} release
A, representative Ca^{2+} transients elicited by either voltage (left) or exposure to 30 mM caffeine (right). Transients were obtained from one representative control (top) and one representative CGRP-treated (200 nM, ~4 h) myotube (bottom). The vertical calibration bar indicates initiation of the depolarizing pulse (30 ms to +70 from a holding potential of −80 mV). Caffeine was applied (hatched bar) ~20 s thereafter (//). Horizontal calibration bar represents 0.2 s (left) and 0.8 s (right). *B*, average peak amplitude of voltage- (left) and caffeine-induced (right) Ca^{2+} transients. Results were obtained from 13 control and 10 CGRP-treated (~4 h) myotubes. The treatment with CGRP consisted of one, two, or three aliquots (delivered every 2 h) of 100 nM CGRP. $^{*}P < 0.005$, $\#P < 0.001$; compared to control.

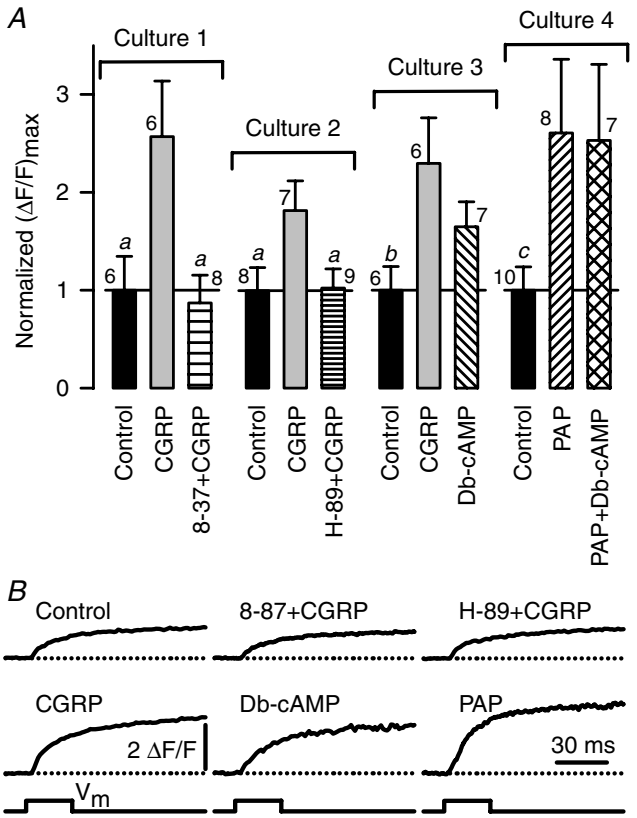

Figure 7. CGRP enhancement of voltage-gated Ca^{2+} release is mediated by a CGRP1 receptor activated cAMP/PKA signalling pathway
A, effects of CGRP and other compounds on the amplitude of voltage-gated SR Ca^{2+} release ($(\Delta F/F)_{max}$). Values of $(\Delta F/F)_{max}$ were determined from the end of 30 ms depolarizating pulses to saturating voltages (+30 to +70 mV). Four different experimental series were carried out (Cultures 1–4). The average $(\Delta F/F)_{max}$ for each control group was (mean ± S.E.M.): 0.6 ± 0.2, 1.2 ± 0.3, 0.8 ± 0.2 and 0.7 ± 0.2; for Cultures 1, 2, 3 and 4, respectively. All $(\Delta F/F)_{max}$ values for each culture were divided by the mean value obtained from the corresponding control group (normalized $(\Delta F/F)_{max}$). The number of myotubes that were investigated in each experimental condition is indicated near to the corresponding error bar. Both the CGRP1 receptor antagonist $CGRP_{8\text{-}37}$ (8–37; 3 μM) and the PKA inhibitor (H-89; 10 μM) were added 60 min prior to CGRP exposure and remained present thereafter. For Culture 4, the cAMP analogue, Db-cAMP, was used at a concentration of 0.5 mM and the phosphodiesterase inhibitor, papaverine (PAP), was used at a concentration of 10 μM. Simultaneous treatment with both Db-cAMP and PAP was accomplished by applying the two compounds at the same time (PAP + Db-cAMP). For Cultures 1, 2 and 4, treatments lasted 1 day and CGRP was used at a concentration of 100 nM. In contrast, one, two, or three aliquots (delivered every 2 h) of either 100 nM CGRP or 0.5 mM Db-cAMP (~4 h treatment) were used for Culture 3. $^{a}P < 0.05$ compared to CGRP. $^{b}P < 0.15$ compared to both CGRP and Db-cAMP. $^{c}P < 0.10$ compared to both PAP and PAP + Db-cAMP. Statistical tests (one-way ANOVA) were only performed between groups of the same culture. *B*, examples of Ca^{2+} transients recorded from the experimental conditions described in *A*.

CGRP1 receptors, cAMP, and PKA in mediating these effects. Our results also suggest that CGRP exerts a long-term up-regulation in the number of sarcolemmal DHPRs (1.25-fold increase). Below we discuss the possible physiological relevance of these findings, as well as the potential underlying mechanisms involved.

Molecular mechanisms associated to SR Ca^{2+} release

Our results point to PKA as a critical link in mediating the reported effects. Potentiation of Ca^{2+} release most likely results from an increased SR Ca^{2+} content, since CGRP exposure similarly increased the magnitude of the caffeine-sensitive Ca^{2+} store (Fig. 6). Steady-state SR Ca^{2+} content depends on a balance between Ca^{2+} uptake and Ca^{2+} 'leak' (defined as the efflux of Ca^{2+} under resting conditions). The SR Ca^{2+}-ATPase (SERCA) accounts for the uptake, whereas the molecular identity of the pathway(s) responsible for the leak remains controversial. It is well established that phospholamban (PLB), an intrinsic protein of the SR, inhibits SERCA2, through a physical interaction with the enzyme. Conversely, phosphorylation of PLB by PKA relieves that inhibition (Simmerman & Jones, 1998). Interestingly, both myoblasts and differentiated myotubes express PLB (Stenoien *et al.* 2007) and SERCA2 (Kimura *et al.* 2005). Thus, CGRP might promote SERCA-mediated SR Ca^{2+} uptake via a PKA-mediated phosphorylation of PLB. If that is the case, then increase SERCA activity would account for the observed increase in SR Ca^{2+} content. Further experiments are needed in order to more rigorously test this hypothesis.

Molecular mechanisms associated to DHPR expression

Our study shows that CGRP increases both L-type Ca^{2+} current density and DHPR charge movement to a similar extent (~25%), without significantly altering their corresponding voltage dependence of activation. Thus, CGRP treatment increases the expression of functional DHPRs within the sarcolemma. This effect could be explained either by CGRP (a) stimulating the insertion of newly formed or preassembled DHPRs into the sarcolemma or (b) inhibiting the degradation rate of sarcolemmal DHPRs. A genomic mechanism is likely to be involved since a significant increase in L-type Ca^{2+} current density is first detected only 24 h after CGRP exposure (~1 day, see Fig. 4). The long-term functional expression of DHPRs is also promoted by Ca^{2+} release through RyR1s (Avila *et al.* 2001). It will therefore be of interest to investigate whether the CGRP treatment enhances DHPR expression through the short-term potentiation of voltage-gated SR Ca^{2+} release.

Interestingly, it has been reported that the downstream signalling molecule of CGRP1 stimulation, cAMP, significantly increases the density of sarcolemmal DHPRs (Schmid *et al.* 1985). Moreover, the transcription rate for the gene encoding skeletal muscle DHPRs (*CACNA1S*) is also stimulated via the cAMP-response element binding protein (CREB, Zheng *et al.* 2002). Thus, CGRP could stimulate transcription of *CACNA1S*, by acting through cAMP and CREB.

Nevertheless, results from Ray *et al.* (1995) cast doubts on a possible transcriptional mechanism. This is because they found that cAMP does not affect mRNA levels encoding any of the α_{1S}-, α_2-, and β-subunits of the DHPR. Hence, while cAMP increases the number of sarcolemmal DHPRs (Schmid *et al.* 1985), it does not do this through stimulation of *de novo* synthesis (Ray *et al.* 1995). Alternatively, CGRP could inhibit DHPR proteolysis and/or degradation. Recent studies provide indirect experimental support for such an idea. Carrillo *et al.* (2004) found that DHPRs are degraded by calpain, a Ca^{2+}-dependent protease. On the other hand, Navegantes *et al.* (2001) found that cAMP inhibits Ca^{2+}-dependent proteolysis, an effect probably explained by an increased synthesis of calpastatin, which in turn inhibits calpain-dependent proteolysis (Parr *et al.* 2001). Thus, it will be critical for future investigations to determine whether CGRP prevents DHPR degradation, via cAMP, calpastatin and calpain. Other mechanisms than enhanced gene transcription and reduced protein degradation may also be involved in the observed increase in the density of sarcolemmal DHPRs.

Physiological relevance

Expression level of CGRP in motor neurons is elevated during embryonic development, tends to decrease in parallel with maturation of the neuromuscular junction, and is essentially undetectable in adults (Matteoli *et al.* 1990). Nevertheless, expression level of CGRP in adult motor neurons is greatly increased in response to physiological and pathophysiological stimuli, including exercise (Homonko & Theriault, 1997), trophic factors (Piehl *et al.* 1998), muscle inactivity (Sala *et al.* 1995), and neuromuscular blockade (Sala *et al.* 1995; Piehl *et al.* 1998). Thus, CGRP is thought to participate in neuromuscular junction regeneration in adults. In keeping with this, it has been suggested that CGRP stimulates myoblast fusion (Noble *et al.* 1993) and the subsequent myotube differentiation (Okazaki *et al.* 1996). Moreover, CGRP is also detected in skeletal muscle (Jiang *et al.* 2003), suggesting the presence of a possible autocrine role.

CGRP has been suggested to stimulate myoblast fusion (Noble *et al.* 1993). However, we did not find systematic effects of CGRP treatment on membrane capacitance

(C_m), which would have suggested significant alterations in myotube size. Specifically, average C_m values for 3 day control and CGRP-treated myotubes were 184 ± 29 pF and 181 ± 33 pF, respectively ($P = 0.94$). We should take into account that C_m values are strongly influenced by investigator sampling bias. Thus, this does not mean that myotubes were not larger on average in CGRP-treated myotubes. Another possible explanation for this apparent contradiction relies on the fact that CGRP treatment was given 3 days after initiation of differentiation and that treatment was limited to a maximum of only 3 days. In contrast, Noble *et al.* (1993) exposed myotubes to CGRP for 11 days.

On the other hand, our results are consistent with the previous observation that CGRP accelerates myotube differentiation (Okazaki *et al.* 1996). Specifically, this study found that expression levels of myogenic regulatory factors (myogenin and Myf-5), myoglobin content and creatine kinase activity occurred earlier and in larger amounts in CGRP-treated myotubes compared to controls (Okazaki *et al.* 1996).

In summary, our data support the notion that CGRP stimulates development of EC coupling by acting through CGRP1 receptors and the cAMP/PKA signalling pathway. Specifically, CGRP increases voltage-gated SR Ca^{2+} release within hours and the density of sarcolemmal DHPRs in days. Stimulation of voltage-gated Ca^{2+} release seems to result from a quantitatively similar increase in releasable SR Ca^{2+} content. This interpretation is supported by the finding that CGRP enhances SR Ca^{2+} content, without significantly altering the voltage dependence of L-current conductance, DHPR charge movements, or Ca^{2+} release. These effects are most prominent early during myotube maturation. Whether these effects also occur in muscle regeneration remains to be elucidated.

References

Andersen SL & Clausen T (1993). Calcitonin gene-related peptide stimulates active Na^+-K^+ transport in rat soleus muscle. *Am J Physiol Cell Physiol* **264**, C419–C429.

Avila G & Dirksen RT (2005). Rapamycin and FK506 reduce skeletal muscle voltage sensor expression and function. *Cell Calcium* **38**, 35–44.

Avila G, O'Connell KM, Groom LA & Dirksen RT (2001). Ca^{2+} release through ryanodine receptors regulates skeletal muscle L-type Ca^{2+} channel expression. *J Biol Chem* **276**, 17732–17738.

Beam KG & Franzini-Armstrong C (1997). Functional and structural approaches to the study of excitation-contraction coupling. *Methods Cell Biol* **52**, 283–306.

Boudreau-Lariviere C & Jasmin BJ (1999). Calcitonin gene-related peptide decreases expression of acetylcholinesterase in mammalian myotubes. *FEBS Lett* **444**, 22–26.

Carrillo E, Galindo JM, Garcia MC & Sanchez JA (2004). Regulation of muscle Cav1.1 channels by long-term depolarization involves proteolysis of the alpha1s subunit. *J Membr Biol* **199**, 155–161.

Chiba T, Yamaguchi A, Yamatani T, Nakamura A, Morishita T, Inui T, Fukase M, Noda T & Fujita T (1989). Calcitonin gene-related peptide receptor antagonist human CGRP-(8–37). *Am J Physiol Endocrinol Metab* **256**, E331–E335.

Dirksen RT (2002). Bi-directional coupling between dihydropyridine receptors and ryanodine receptors. *Front Biosci* **7**, d659–d670.

Fernandez HL, Chen M, Nadelhaft I & Durr JA (2003). Calcitonin gene-related peptides: their binding sites and receptor accessory proteins in adult mammalian skeletal muscles. *Neuroscience* **119**, 335–345.

Fontaine B, Klarsfeld A, Hokfelt T & Changeux JP (1986). Calcitonin gene-related peptide, a peptide present in spinal cord motoneurons, increases the number of acetylcholine receptors in primary cultures of chick embryo myotubes. *Neurosci Lett* **71**, 59–65.

Hay DL, Poyner DR & Smith DM (2003). Desensitisation of adrenomedullin and CGRP receptors. *Regul Pept* **112**, 139–145.

Homonko DA & Theriault E (1997). Calcitonin gene-related peptide is increased in hindlimb motoneurons after exercise. *Int J Sports Med* **18**, 503–509.

Jiang JX, Choi RC, Siow NL, Lee HH, Wan DC & Tsim KW (2003). Muscle induces neuronal expression of acetylcholinesterase in neuron-muscle co-culture: transcriptional regulation mediated by cAMP-dependent signaling. *J Biol Chem* **278**, 45435–45444.

Juaneda C, Dumont Y & Quirion R (2000). The molecular pharmacology of CGRP and related peptide receptor subtypes. *Trends Pharmacol Sci* **21**, 432–438.

Kimura T, Nakamori M, Lueck JD, Pouliquin P, Aoike F, Fujimura H, Dirksen RT, Takahashi MP, Dulhunty AF & Sakoda S (2005). Altered mRNA splicing of the skeletal muscle ryanodine receptor and sarcoplasmic/endoplasmic reticulum Ca^{2+}-ATPase in myotonic dystrophy type 1. *Hum Mol Genet* **14**, 2189–2200.

Lu B, Fu WM, Greengard P & Poo MM (1993). Calcitonin gene-related peptide potentiates synaptic responses at developing neuromuscular junction. *Nature* **363**, 76–79.

Marty I, Robert M, Villaz M, De Jongh K, Lai Y, Catterall WA & Ronjat M (1994). Biochemical evidence for a complex involving dihydropyridine receptor and ryanodine receptor in triad junctions of skeletal muscle. *Proc Natl Acad Sci U S A* **91**, 2270–2274.

Matteoli M, Balbi S, Sala C, Chini B, Cimino M, Vitadello M & Fumagalli G (1990). Developmentally regulated expression of calcitonin gene-related peptide at mammalian neuromuscular junction. *J Mol Neurosci* **2**, 175–184.

Mejia-Luna L & Avila G (2004). Ca^{2+} channel regulation by transforming growth factor-β1 and bone morphogenetic protein-2 in developing mice myotubes. *J Physiol* **559**, 41–54.

Melzer W, Herrmann-Frank A & Luttgau HC (1995). The role of Ca^{2+} ions in excitation-contraction coupling of skeletal muscle fibres. *Biochim Biophys Acta* **1241**, 59–116.

Mulle C, Benoit P, Pinset C, Roa M & Changeux JP (1988). Calcitonin gene-related peptide enhances the rate of desensitization of the nicotinic acetylcholine receptor in cultured mouse muscle cells. *Proc Natl Acad Sci U S A* **85**, 5728–5732.

Navegantes LC, Resano NM, Migliorini RH & Kettelhut IC (2001). Catecholamines inhibit Ca^{2+}-dependent proteolysis in rat skeletal muscle through β_2-adrenoceptors and cAMP. *Am J Physiol Endocrinol Metab* **281**, E449–E454.

New HV & Mudge AW (1986). Calcitonin gene-related peptide regulates muscle acetylcholine receptor synthesis. *Nature* **323**, 809–811.

Noble BS, McMillan DN & Maltin CA (1993). Calcitonin gene related peptide stimulates differentiation of neonatal rat myogenic cultures. *Growth Regul* **3**, 245–248.

Okazaki S, Kawai H, Arii Y, Yamaguchi H & Saito S (1996). Effects of calcitonin gene-related peptide and interleukin 6 on myoblast differentiation. *Cell Prolif* **29**, 173–182.

Parr T, Sensky PL, Bardsley RG & Buttery PJ (2001). Calpastatin expression in porcine cardiac and skeletal muscle and partial gene structure. *Arch Biochem Biophys* **395**, 1–13.

Piehl F, Hammarberg H, Hokfelt T & Cullheim S (1998). Regulatory effects of trophic factors on expression and distribution of CGRP and GAP-43 in rat motoneurons. *J Neurosci Res* **51**, 1–14.

Ray A, Kyselovic J, Leddy JJ, Wigle JT, Jasmin BJ & Tuana BS (1995). Regulation of dihydropyridine and ryanodine receptor gene expression in skeletal muscle. Role of nerve, protein kinase C, and cAMP pathways. *J Biol Chem* **270**, 25837–25844.

Rios E & Brum G (1987). Involvement of dihydropyridine receptors in excitation-contraction coupling in skeletal muscle. *Nature* **325**, 717–720.

Rossi SG, Dickerson IM & Rotundo RL (2003). Localization of the calcitonin gene-related peptide receptor complex at the vertebrate neuromuscular junction and its role in regulating acetylcholinesterase expression. *J Biol Chem* **278**, 24994–25000.

Sakaguchi M, Inaishi Y, Kashihara Y & Kuno M (1991). Release of calcitonin gene-related peptide from nerve terminals in rat skeletal muscle. *J Physiol* **434**, 257–270.

Sala C, Andreose JS, Fumagalli G & Lomo T (1995). Calcitonin gene-related peptide: possible role in formation and maintenance of neuromuscular junctions. *J Neurosci* **15**, 520–528.

Schmid A, Renaud JF & Lazdunski M (1985). Short term and long term effects of β-adrenergic effectors and cyclic AMP on nitrendipine-sensitive voltage-dependent Ca^{2+} channels of skeletal muscle. *J Biol Chem* **260**, 13041–13046.

Schneider MF & Chandler WK (1973). Voltage dependent charge movement of skeletal muscle: a possible step in excitation-contraction coupling. *Nature* **242**, 244–246.

Simmerman HK & Jones LR (1998). Phospholamban: protein structure, mechanism of action, and role in cardiac function. *Physiol Rev* **78**, 921–947.

Stenoien DL, Knyushko TV, Londono MP, Opresko LK, Mayer MU, Brady ST, Squier TC & Bigelow DJ (2007). Cellular trafficking of phospholamban and formation of functional sarcoplasmic reticulum during myocyte differentiation. *Am J Physiol Cell Physiol* **292**, C2084–2094.

Takami K, Hashimoto K, Uchida S, Tohyama M & Yoshida H (1986). Effect of calcitonin gene-related peptide on the cyclic AMP level of isolated mouse diaphragm. *Jpn J Pharmacol* **42**, 345–350.

Takami K, Kawai Y, Uchida S, Tohyama M, Shiotani Y, Yoshida H, Emson PC, Girgis S, Hillyard CJ & MacIntyre I (1985). Effect of calcitonin gene-related peptide on contraction of striated muscle in the mouse. *Neurosci Lett* **60**, 227–230.

Tanabe T, Beam KG, Powell JA & Numa S (1988). Restoration of excitation-contraction coupling and slow calcium current in dysgenic muscle by dihydropyridine receptor complementary DNA. *Nature* **336**, 134–139.

Uchida S, Yamamoto H, Iio S, Matsumoto N, Wang XB, Yonehara N, Imai Y, Inoki R & Yoshida H (1990). Release of calcitonin gene-related peptide-like immunoreactive substance from neuromuscular junction by nerve excitation and its action on striated muscle. *J Neurochem* **54**, 1000–1003.

Zheng Z, Wang ZM & Delbono O (2002). Insulin-like growth factor-1 increases skeletal muscle dihydropyridine receptor α1S transcriptional activity by acting on the cAMP-response element-binding protein element of the promoter region. *J Biol Chem* **277**, 50535–50542.

Acknowledgements

We would like to thank Dr Robert T. Dirksen for providing helpful comments for improving the manuscript. We also thank Esperanza Jiménez and Mario Rodriguez for technical assistance. This work was partially supported by a CONACyT grant to GA (39512). CIA and RR-M received graduate student fellowships granted by CONACyT.